



Numerical and experimental study on thermal performance of a novel shell and helically coiled tube heat exchanger design with integrated rings and discs

Alper Güngör^{a,b,*}, Ataollah Khanlari^c, Adnan Sözen^d, Halil Ibrahim Variyenli^d

^a Natural and Applied Sciences Institute, Gazi University, Ankara, Türkiye

^b The Scientific and Technological Research Council of Turkey, Ankara, Türkiye

^c Department of Mechanical Engineering, Faculty of Engineering, Tarsus University, Tarsus, Mersin, Türkiye

^d Energy Systems Engineering, Gazi University, Ankara, Türkiye

ARTICLE INFO

Keywords:

Heat exchanger
Shell and helically coiled tube
Circular baffles
CFD simulation
Experimental investigation

ABSTRACT

Shell and Helically Coiled Tube Heat Exchangers (SHCTHEXs) are utilized in energy conversion applications in industry and in various engineering systems. They are generally composed of a helically coiled tube and a shell covering it. This coiled structure of tubes, provides better heat transfer and takes less space. There is an ongoing interest in research on this type of heat exchangers. In this study, a new design was created modifying a simple type of conventional shell and helically coiled heat exchanger, by integrating discs and rings. These rings and discs were attached to the helically coiled tubes with the aim of performing as baffles restricting the shell side flow and creating turbulence. The thermal performance of a conventional heat exchanger was improved by this modification. The study was carried out both numerically and experimentally. At first step, two SHCTHEXs, one conventional; one modified, were designed with same overall geometric dimensions. Then created solid models were numerically simulated with same boundary conditions using ANSYS Fluent. Simulations were performed with various flow rates and the results were reported. According to the simulations, compared to the conventional one, with the modified heat exchanger 7.1% increase in average amount of heat transfer rate and around 20% increase in overall heat transfer coefficient were obtained. With the promising results taken by simulations, the modified heat exchanger was fabricated with the same dimensions and it was experimentally tested with same conditions in laboratory to verify the simulation results. Experimental results were in harmony with the simulations with little differences. The average differences between simulation and experimental values in terms of average amount of heat transfer rate were obtained as 2.4% for 3 l/min hot fluid flow rate and 3.5% for 4 l/min hot fluid flow rate. Overall heat transfer coefficient of modified SHCTHEX with circular baffles achieved in the range of 1050–1400 W/m²K. General outcomes of this study exhibited successful design of baffled SHCTHEX.

1. Introduction

Heat exchangers are widely used in industry to transfer heat from one energy source to another and their performance directly affects the system efficiency. A common type of heat exchanger in industry is called “Shell and Helically Coiled Heat Exchanger”. This heat exchanger is designed to have helically coiled tube/tubes inside a shell. Helically coiled tube structure creates a secondary flow inside the tubes because of the centrifugal force, which in turn increases the amount of heat transfer to the other fluid and also this construction occupies less space compared to straight tubes [1].

Shell and helically coiled tube heat exchangers (SHCTHEXs) are utilized in various applications at chemistry, manufacturing, food and beverage industries; at waste heat recovery systems, thermal power plants etc. [2]. Research on shell and helically coiled heat exchangers is still going on and there are many studies in literature. Some of the most relevant and up to date studies are mentioned below.

Etghani and Hosseini Baboli [3] proposed a model to investigate the influence of some geometrical parameters such as coil diameter and pitch size on thermal and flow behavior of a SHCTHEX. Jamshidi et al. [4] experimentally examined the influence of factors like coil diameter and coil pitch at different flow rates and determined the optimum geometrical parameters for various working conditions. Andrzejczyk

* Corresponding author. Natural and Applied Sciences Institute, Gazi University, Ankara, Türkiye.
E-mail address: alprngr@gmail.com (A. Güngör).

<https://doi.org/10.1016/j.ijthermalsci.2022.107781>

Received 25 February 2022; Received in revised form 31 May 2022; Accepted 28 June 2022

Available online 3 August 2022

1290-0729/© 2022 Elsevier Masson SAS. All rights reserved.

Nomenclature			
A	Area at contact region where heat transfer occurs (m^2)	U	Overall heat transfer coefficient ($W/m^2.K$)
c_p	Heat capacity at constant pressure ($kJ/kg.K$)	V	Velocity (m/s)
C	Heat capacity rate (W/K)	\vec{v}	Overall velocity vector (m/s)
$D_{t,o}$	Outer diameter of coiled tube (m)	<i>Greek letters</i>	
$D_{t,i}$	Inner diameter of coiled tube (m)	ΔT_{LMTD}	Logarithmic mean temperature difference (K)
D_{coil}	Diameter of coil (m)	ε	Effectiveness
D_{shell}	Diameter of shell (m)	μ	Dynamic viscosity ($Pa.s$)
D_h	Hydraulic diameter (m)	ρ	Density (kg/m^3)
De	Dean Number	δ	Thickness (mm)
E	Energy (J)	<i>Subscripts</i>	
h	Coefficient of heat transfer ($W/m^2.K$)	<i>in</i>	Inlet
k	Conductivity ($W/m.K$)	<i>i</i>	Inner
L	Length (m)	<i>o</i>	Outer
\dot{m}	Mass flow rate (kg/s)	<i>out</i>	Outlet
Nu	Nusselt Number	<i>t</i>	Tube
p	Pressure (Pa)	<i>Abbreviations</i>	
Pr	Prandtl Number	<i>CFD</i>	Computational Fluid Dynamics
Re	Reynolds Number	<i>LMTD</i>	Logarithmic Mean Temperature Difference
T	Temperature (K)	<i>lpm</i>	Liters per minute
\dot{Q}	Heat transfer rate (W)	<i>SHCTHEX</i>	Shell and Helically Coiled Heat Exchanger

and Muszynski [5] empirically surveyed the impact of applying continuous core-baffle modification on thermal and flow characteristics of a SHCTHEX. Alimoradi [6] employed exergy methodology to investigate the overall characteristics of SHCTHEXs. In another work, Alimoradi [7] experimentally and numerically analyzed thermal effectiveness and its relation with NTU in SHCTHEXs. Hardik et al. [8] fabricated a SHCTHEX and investigated the impact of geometrical factors on thermohydraulic behavior of the SHCTHEX. Ramesh et al. [9] empirically tested a SHCTHEX to specify its thermal performance in absorption refrigeration system. Maghrabie et al. [10] experimentally investigated the effect of inclination angle on the effectiveness of a SHCTHEX. In another study, Maghrabie et al. [11] analyzed the influences of inclination angle and using various nanofluids on the thermal performance of a SHCTHEX. Khorasani et al. [12] experimentally surveyed the impact of bubble injection on the flow and thermal characteristics of a SHCTHEX. Solanki and Kumar [13] experimentally studied the impact of using dimpled helically coiled tube on the overall behavior of a SHCTHEX to be utilized in condensation of R-134a. Their results exhibited the successful utilization of dimpled tube in terms of thermal performance.

There are some methods available to improve the thermal performance of thermal systems like heat exchangers [14,15]. One of the widely utilized methods is integrating fins to increase heat transfer surface area and consequently improve heat transfer rate [16–19]. In a study, Andrzejczyk et al. [20] empirically analyzed the influence of utilizing various types of fins and baffles on the total efficiency of a SHCTHEX. Panahi and Zamzamin [21] utilized helical wire turbulator to increase turbulence intensity and consequently improving the thermal performance of a SHCTHEX. Their experimental findings indicated significant effect of wire turbulator modification on the thermal efficiency of the SHCTHEX. Tuncer et al. [2] developed a new type of SHCTHEX by adding an additional tube to the shell side of the heat exchanger with the aim of directing the flow to the helically coiled tube to enhance heat transfer. In another study, Tuncer et al. [22] utilized longitudinal fins to obtain more improvement for the heat transfer in the developed SHCTHEX. Solanki and Kumar [23] compared utilization of smooth and dimpled helically coiled tube in the SHCTHEX. Their results showed that using dimpled helically coiled tube can increase heat transfer rate. Andrzejczyk and Muszynski [24] proposed different types

of baffle modifications to enhance the thermal efficiency of the SHCTHEX.

In addition to the experimental studies, there are some important researches available in the literature that numerically investigated different systems [25–27]. Numerical methods like Computational Fluid Dynamics (CFD) makes it possible to study flow and thermal behavior of energy systems like heat exchangers before manufacturing them [28–30]. In a study, Miansari et al. [31] numerically investigated grooves effects on the overall efficiency of a SHCTHEX. Kumar et al. [32] modeled micro-finned helically coiled tubes to determine thermal and flow behavior. Abu-Hamdeh et al. [33] numerically modeled flow and thermal behavior of helically coiled tube heat exchangers by employing exergy method. Omidi et al. [34] simulated a SHCTHEX to specify the impact of utilizing tubes with lobed cross sections on the thermal and flow characteristics. Wang et al. [35] modeled a SHCTHEX to determine its thermohydraulic behavior and compared the obtained results with experimental findings. Mirgolbabaie [36] numerically studied the importance of working conditions and geometrical parameters on the overall behavior of a SHCTHEX. Alimoradi and Veysi [37] simulated heat and flow characteristics in a SHCTHEX and verified the obtained findings with empirical results. Abu-Hamdeh et al. [38] applied CFD technique to investigate overall characteristics of a sector-by-sector helically coiled type heat exchanger.

Analyzing available researches in the literature showed that different types of fins and baffles can be used to improve the thermal efficiency of SHCTHEXs. However, providing appropriate fin and baffle modifications is necessary to increase the overall performance of the SHCTHEXs because of their special design. In the present work, different from related studies, circular baffles (discs and rings) have been integrated over the helically coiled tube in order to guide the flow to the coiled tube with the aim of enhancing the rate of heat transfer. In this context, in the first step of this work, CFD method has been applied to determine the effect of utilizing circular baffles. In the next step, finned SHCTHEX has been manufactured according to the numerical analysis results. Finally, the fabricated baffled SHCTHEX has been tested at different working conditions to determine its performance.

2. Design and simulation

2.1. Geometry

A wide variety of shell and helical coiled tube heat exchangers are available in the literature. In this study, one very common configuration of these designs was chosen and a solid model of it was created utilizing ANSYS Geometry Module (Fig. 1a). The heat exchangers studied in this work is oriented horizontally, has a right handed helically coiled tube inside, fluid enters to shell from the bottom; leaves from the top and other fluid is circulated within the helically coiled tubes. Keeping the same dimensional values, the conventional design was improved by integrating rings and discs as seen in Fig. 1b. The main aim of adding baffles is guiding the cold fluid to the helically coiled tube in order to enhance heat transfer rate.

Since this study aims to investigate the improvement potential of a new design, values of geometric parameters was kept equal for both designs to be able to make a reliable comparison. Mutual geometric parameters are shown in Fig. 2 and their values are presented in Table 1.

The general dimensional values were determined according to the previous works of authors and the test rig available at the laboratory ([2, 22,39]. Tube diameter was determined according to the copper tubes

available at the market. The most suitable one (3/8") was chosen.

The modified heat exchanger has rings and discs integrated which act as baffles creating more turbulence at shell side and make it possible to direct the flow over the helically coiled tube. The dimensions of rings and discs used are presented in Fig. 3 and their locations in the modified

Table 1

Geometrical parameters of analyzed SHCTHEXs.

Parameters	Dimensions
Length of Shell, L_{shell}	340 mm
Length of Helically Coiled Tube, L_{coil}	300 mm
Shell Diameter, D_{shell}	140 mm
Coil Diameter, D_{coil}	100 mm
Coil Pitch, p (number of turns)	16,67 mm (18 full turns)
Tube Outer Diameter, $D_{t,o}$	9.52 mm (3/8")
Tube Inner Diameter, $D_{t,i}$	8.52 mm
Shell side Inlet and Outlet Diameters	12 mm

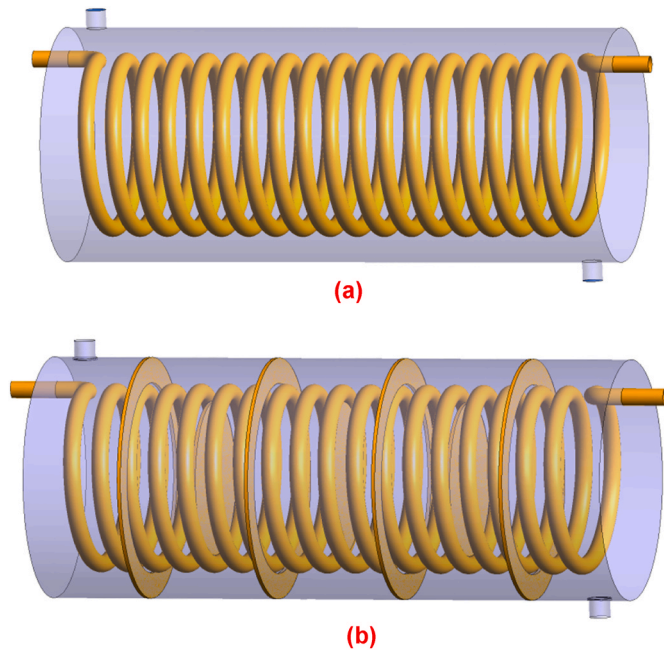


Fig. 1. Geometries of SHCTHEXs; a) Conventional, b) Modified with baffles.

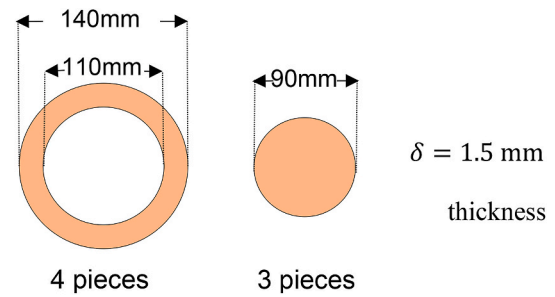


Fig. 3. Dimensions of designed rings and discs.

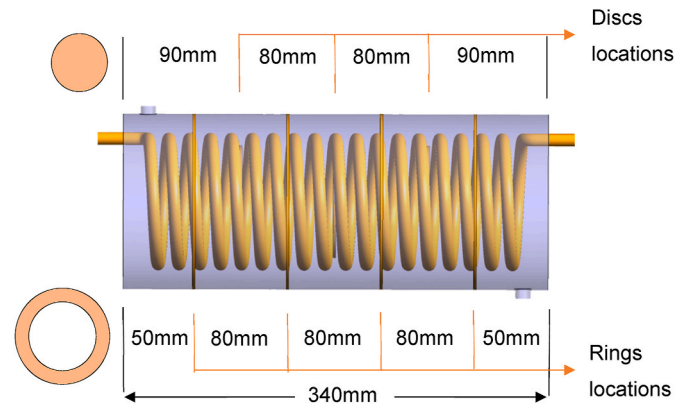


Fig. 4. Locations of discs and rings.

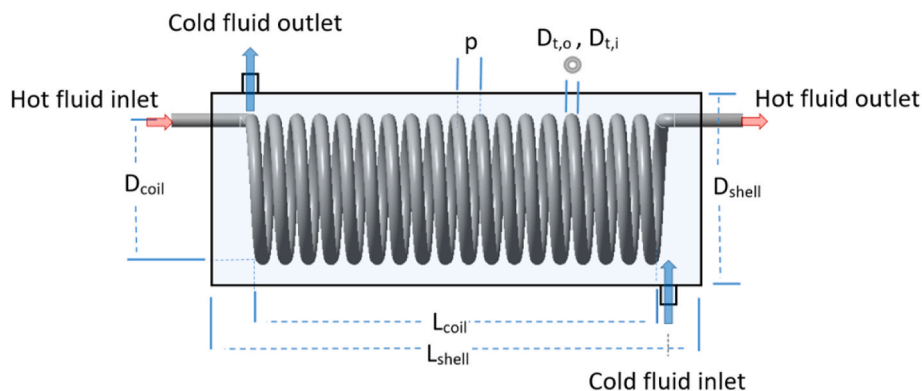


Fig. 2. Geometrical parameters of analyzed SHCTHEXs and flow configurations.

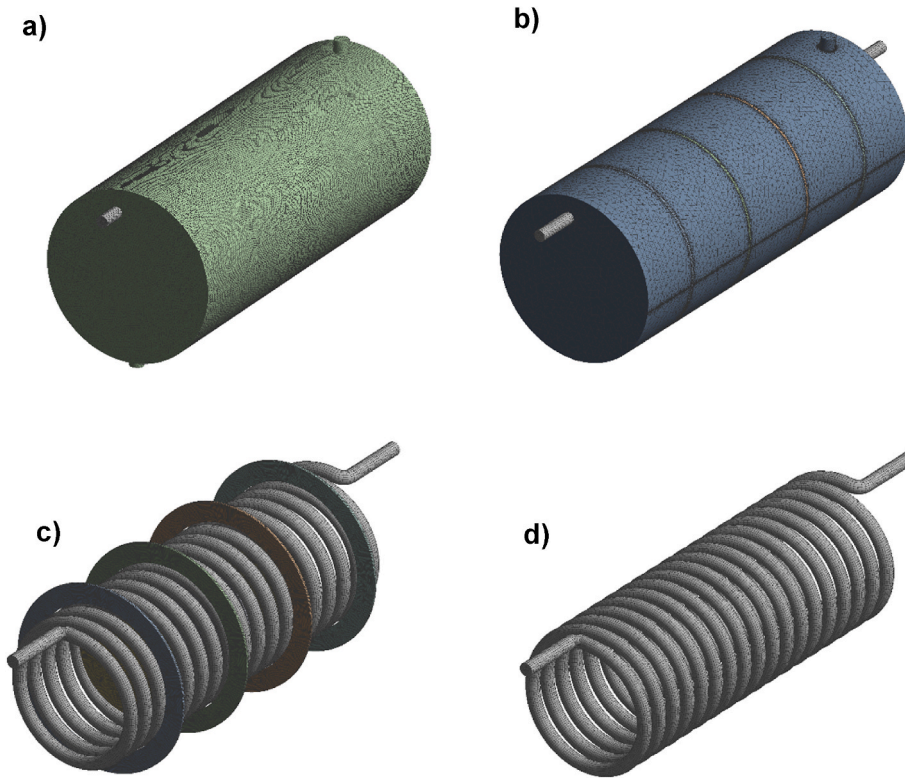


Fig. 5. Generated mesh details for simulations; a) Conventional heat exchanger, b) Shell side's fluid and helically coiled tube with baffles, c) Helically coiled tube with baffles, d) Helically coiled tube.

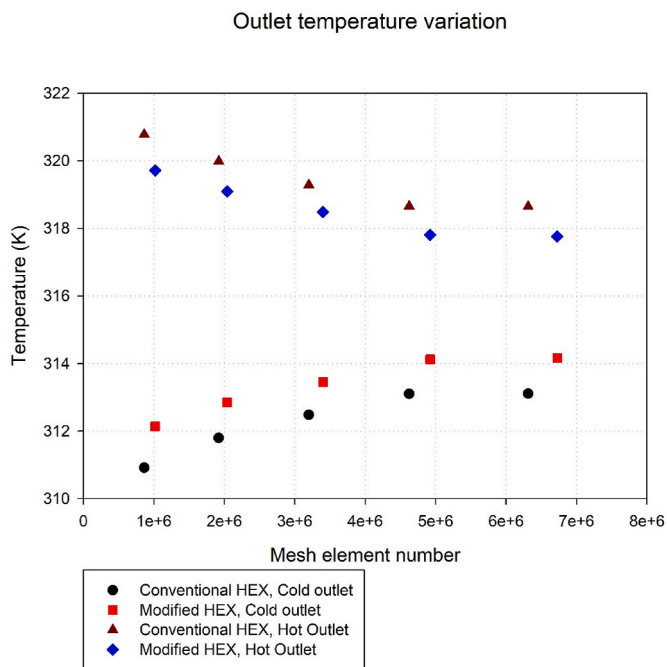


Fig. 6. Variation of outlet temperature in SHCTHEXs via mesh elements number.

SHCTHEX are shown in Fig. 4. The solid models of SHCTHEX were created as explained above using ANSYS Geometry Module and prepared for meshing before simulations.

2.2. Meshing

CFD (Computational Fluid Dynamics) technique provides an opportunity to simulate a systems performance with varying conditions. The CFD approach is a powerful tool for understanding and eliciting the response of a system and is often used in engineering applications involving different energy systems. In order to perform computational fluid dynamics analyses, a proper mesh structure has to be established. ANSYS Mesh Module was used for meshing the SHCTHEX models created in this study.

There are many criteria for ensuring an appropriate mesh structure such as skewness and aspect ratio. ANSYS Fluent guidelines recommend a maximum skewness value of 0.95; an average skewness value below 0.35 and maximum aspect ratio value below 35. In this study, mesh independence analyzes are performed before the simulations to determine the appropriate mesh structure which would be suitable and efficient to solve the problem. Fig. 6 illustrates variation of outlet temperatures in conventional SHCTHEX and modified SHCTHEX with baffles via mesh elements number. Mesh independence analyzes showed that some elements number about 6 million elements were enough and after that very little differences were noted. However, adding baffles to the SHCTHEX increased mesh elements number slightly. Fig. 5 represents utilized mesh for modified SHCTHEX at different zones which were generated considering the criteria explained above. In addition, Table 2 shows details of generated meshes for two SHCTHEXs. As it is clearly seen in Table 2, selected mesh structures for numerical simulations of SHCTHEXs have high qualities considering skewness and aspect ratio quality factors.

2.3. CFD analysis

CFD approach is a powerful method to evaluate a system's behavior in an approximate manner to reality. This method decreases the amount of time and effort to reveal a systems outcome at different working

Table 2
Details of generated meshes for two SHCTHEXs.

Heat exchanger type	Mesh elements number	Mesh nodes number	Maximum skewness value	Average skewness value	Maximum aspect ratio value	Average aspect ratio value
Conventional SHCTHEX	6,313,232	2,431,447	0.84	0.19	14.53	1.87
Modified SHCTHEX with baffles	6,728,578	1,608,290	0.87	0.28	13.71	1.97

conditions. A system could be analyzed over and over at various conditions and significant information about the system's thermal and flow behavior can be obtained. After obtaining the simulation outcomes, it is possible to fabricate the system with desired specifications. In this regard CFD simulations were conducted considering two designs for SHCTHEX to determine the impact of adding baffles including rings and discs. The required governing formulas for CFD analysis are given as follows [40–42]:

Continuity Eq,

$$\nabla \cdot (\rho \cdot \vec{v}) = 0 \quad (1)$$

Momentum Eq,

$$\nabla \cdot (\rho \cdot \vec{v} \cdot \vec{v}) = -\nabla p + \nabla \cdot \left(\mu \left[(\nabla \vec{v} + \nabla \vec{v}^T) - \frac{2}{3} \nabla \cdot \vec{v} I \right] \right) \quad (2)$$

Energy Eq,

$$\nabla \cdot (\vec{v} (\rho E + p)) = \nabla \cdot k_{eff} \nabla T - h \vec{J} + \left(\mu \left[(\nabla \vec{v} + \nabla \vec{v}^T) - \frac{2}{3} \nabla \cdot \vec{v} I \right] \cdot \vec{v} \right) \quad (3)$$

According to the initial analysis numerical, inside the SHCTHEX, it is expected to see turbulent flow in the flow field of this type of complex heat exchanger. **$k - \epsilon$ turbulence model provides a proper approach to turbulence phenomenon inside the flow field and various options of this model are extensively applied for different energy systems like heat exchangers [43–45]. In this context $k - \epsilon$ turbulence model was utilized in the CFD analysis step of the present research and this model could be given using the following equations where k shows turbulent kinetic energy and ϵ denotes the rate of dissipation in kinetic energy [16,46,47]:**

$$\rho \frac{\partial}{\partial x_i} (k v_i) = \frac{\partial}{\partial x_j} \left[\left(\frac{\mu + \mu_t}{\sigma_k} \right) \frac{\partial k}{\partial x_j} \right] + G_k + G_b - \rho \epsilon - Y_M + S_k \quad (4)$$

$$\rho \frac{\partial}{\partial x_i} (\epsilon v_i) = \frac{\partial}{\partial x_j} \left[\left(\frac{\mu + \mu_t}{\sigma_\epsilon} \right) \frac{\partial \epsilon}{\partial x_j} \right] + C_{1\epsilon} \frac{\epsilon}{k} (G_k + C_{3\epsilon} G_b) - C_{2\epsilon} \rho \frac{\epsilon^2}{k} + S_\epsilon \quad (5)$$

In Eq. (4), G_k shows the turbulence kinetic energy production due to the velocity difference, G_b denotes the turbulence kinetic energy production because of the buoyancy effect, S_ϵ and S_k illustrate source terms, Y_M illustrates the impact of the fluctuating expansion in compressible turbulence to the overall dissipation, and also $C_{3\epsilon}$, $C_{2\epsilon}$ and $C_{1\epsilon}$ are constants. In addition, σ_k and σ_ϵ are the turbulent Prandtl numbers for k and ϵ , respectively.

In the above equations the turbulent viscosity (μ_t) could be gained by combination of ϵ and k as:

$$\mu_t = \rho C_\mu \frac{k^2}{\epsilon} \quad (6)$$

where C_μ is a constant.

The model constants $C_{1\epsilon}$, $C_{2\epsilon}$, $C_{3\epsilon}$, C_μ , σ_k , and σ_ϵ have the following values [46]:

$$C_{1\epsilon} = 1.44, C_{2\epsilon} = 1.92, C_{3\epsilon} = 1.0, C_\mu = 0.09, \sigma_k = 1.0, \sigma_\epsilon = 1.3$$

In the material selection section of CFD analysis, copper was applied as material of helically coil part of SHCTHEXs. Also, stainless steel was selected as material of shell side of the SHCTHEXs. Moreover, copper was defined as material for integrated rings and discs. Water was

selected as working fluid in both sides of baffled and conventional SHCTHEXs. In the first step of CFD analysis, inlet temperatures of shell side and coil side were given as 291.65 K and 333.15 K, respectively. Simulations were conducted at 2, 3, 4, 5 and 6 l/min of cold side's flow rate. Also, hot side's flow rate was selected as 3 and 4 l/min. In the simulation part of the present study a steady-state condition was selected to be utilized in analyzing SHCTHEXs. SIMPLEC algorithm was selected to be applied for coupling pressure-velocity in simulation of the SHCTHEXs. Also, second order upwind was preferred in solution of momentum and energy equations in the numerical analysis. In addition, in modeling of both conventional and modified SHCTHEXs **convergence criteria for energy, continuity and velocity were preferred as 10^{-7} , 10^{-5} and 10^{-5} , respectively.**

3. Experimental setup

Based on the promising results obtained from the simulations, an experimental study was also carried out. In order to do that, the designed modified heat exchanger was manufactured with the dimensions described in section 2.1. Fig. 7 shows helically coiled tubes, discs and rings cut from sheet copper and finally discs and rings welded on the tube. This structure was then placed in a shell made of steel. Before integrating the heat exchanger into the test rig, it was tested for leaks to ensure that the sealing was completely obtained. After that, the outer surfaces of the heat exchanger were covered with insulation material and aluminum foil. Then the manufactured heat exchanger was integrated into the test setup in the laboratory.

Fig. 8 shows a view of the utilized experimental setup. In addition, Fig. 9 represents a schematic diagram of test setup and utilized devices. Hot water was stored in hot water tank with integrated electrical heater with a dimmer switch for temperature control. It was pumped into the heat exchanger's helically coiled tubes and circulated back into hot water tank. Cold water entered into shell side of the heat exchanger and it was discharged to drain at the outlet. The flow rates were controlled with valves and measured by flow meters. Steady state conditions were obtained and sustained during the experiments. All necessary pipes and equipment were insulated with insulation materials. With this setup, experiments are carried out at different flow rates as in simulations. For each flow rate combination experiments are performed three times. The temperatures at inlets and outlets were measured and stored by a data logger.

Uncertainty analysis is a helpful method to specify the reliability of the obtained empirical outcomes. The experimental uncertainties may be derived from measuring instrument type, calibration of measuring instrument, reading errors, connection types of measuring devices and test conditions [48]. The overall experimental uncertainty could be calculated by applying Eq. (7) [22,49–51]. In addition, experimental uncertainty values for different parameters such as heat transfer rate, overall heat transfer coefficient, ΔT_{LMTD} and heat transfer coefficient could be calculated by utilizing Eqs. 8–11.

$$W_R = \left[\left(\frac{\partial R}{\partial x_1} w_1 \right)^2 + \left(\frac{\partial R}{\partial x_2} w_2 \right)^2 + \dots + \left(\frac{\partial R}{\partial x_n} w_n \right)^2 \right]^{1/2} \quad (7)$$

$$W_Q = \left[\left(\frac{\partial Q}{\partial Q_{cold}} w_{Q_{cold}} \right)^2 + \left(\frac{\partial Q}{\partial Q_{hot}} w_{Q_{hot}} \right)^2 \right]^{1/2} \quad (8)$$

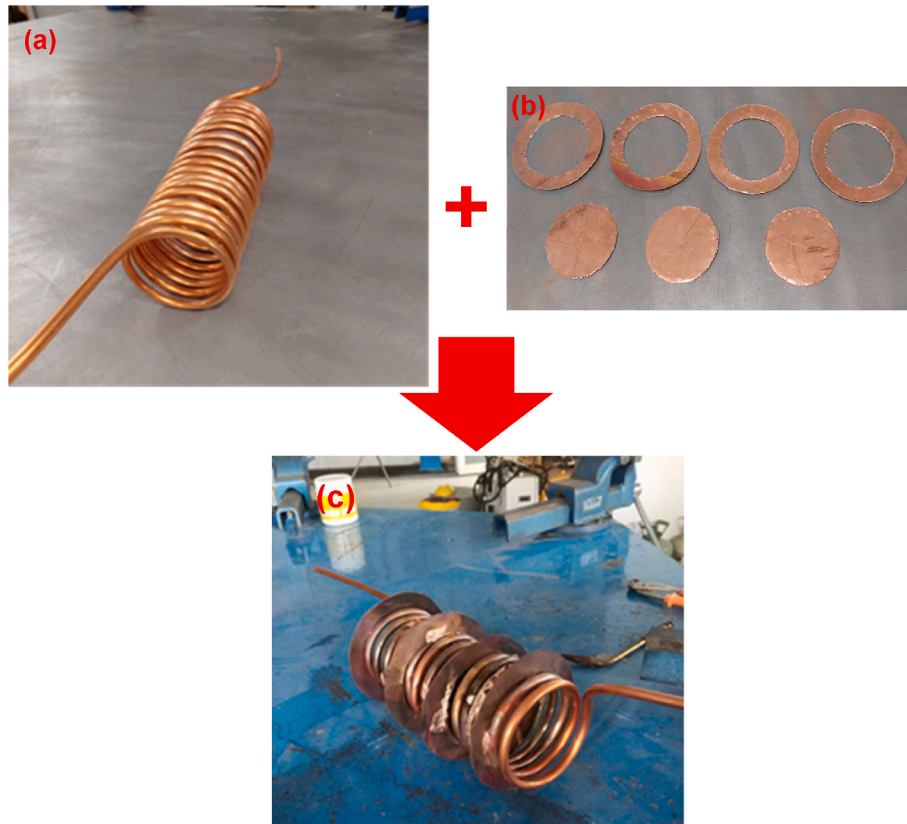


Fig. 7. Manufacturing steps of baffled coil side of modified heat exchanger by using discs and rings.

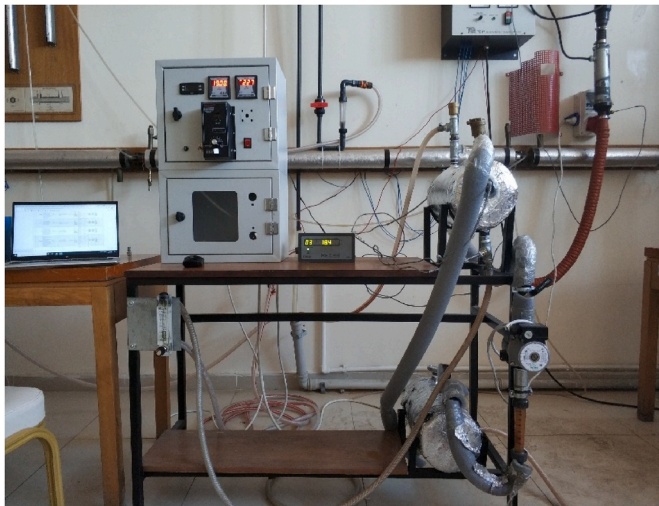


Fig. 8. A view of experimental setup.

$$W_U = \left[\left(\frac{\partial U}{\partial Q} w_Q \right)^2 + \left(\frac{\partial U}{\partial \Delta T_{LMTD}} w_{\Delta T_{LMTD}} \right)^2 \right]^{1/2} \quad (9)$$

$$W_{HTC_{cold}} = \left[\left(\frac{\partial HTC_{cold}}{\partial U} w_U \right)^2 + \left(\frac{\partial HTC_{cold}}{\partial HTC_{hot}} w_{hot} \right)^2 \right]^{1/2} \quad (11)$$

The calculated experimental uncertainties for different parameters of SHCTHEX are illustrated in Table 3. In a related study on SHCTHEX, Tuncer et al. [22] uncertainty values for effectiveness, heat transfer coefficient and mass flow rate obtained as ± 7.62 , ± 6.68 and ± 5.26 , respectively. In another work performed by Khanlari et al. [49,50]; experimental uncertainty value for mass flow rate gained as $\pm 5.36\%$. In a study conducted by Panahi and Zamzamin [21] on a related SHCTHEX, uncertainties for parameters such as effectiveness and heat transfer coefficient calculated as $\pm 10.2\%$ and $\pm 9.17\%$, respectively. Solanki and Kumar [52] experimentally tested a dimpled SHCTHEX and obtained uncertainty values for heat transfer and heat transfer coefficient as 12% and 16%, respectively. Khorasani and Dadvand [53] investigated the performance of a SHCTHEX and obtained experimental uncertainty for effectiveness as ± 9.28 . Moreover, Elshazly et al. [54] tested a SHCTHEX and achieved experimental uncertainty for heat transfer coefficient between the range of 4.7–7.0%. Evaluating the obtained experimental uncertainties for different parameters and comparing them with similar studies available in the literature indicated the reliability of experimental outcomes.

$$W_{\Delta T_{LMTD}} = \left[\left(\frac{\partial \Delta T_{LMTD}}{\partial T_{cold,in}} w_{T_{cold,in}} \right)^2 + \left(\frac{\partial \Delta T_{LMTD}}{\partial T_{cold,out}} w_{T_{cold,out}} \right)^2 + \left(\frac{\partial \Delta T_{LMTD}}{\partial T_{hot,in}} w_{T_{hot,in}} \right)^2 + \left(\frac{\partial \Delta T_{LMTD}}{\partial T_{hot,out}} w_{T_{hot,out}} \right)^2 \right]^{1/2} \quad (10)$$

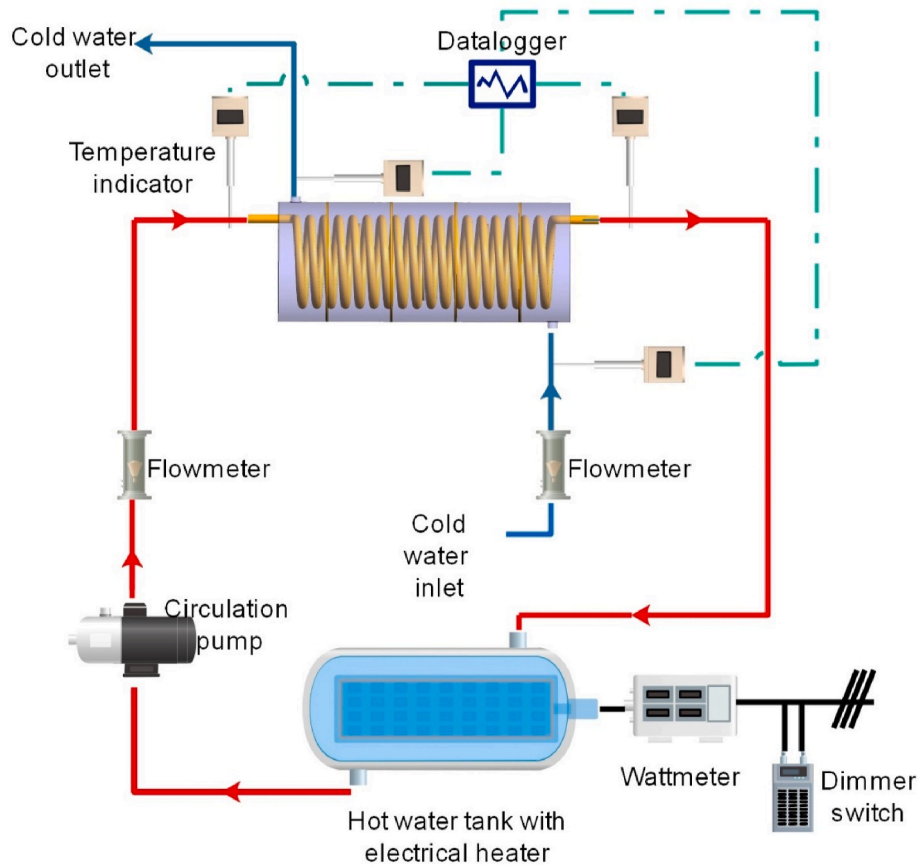


Fig. 9. A schematic diagram of test setup and utilized devices.

Table 3
Calculated experimental uncertainty for different parameters.

Parameter	Unit	Uncertainty value
Temperature	°C	±0.62
\dot{m}	%	±5.13
\dot{Q}	%	±5.20
Heat transfer coefficient	%	±6.54

4. Post analyses calculations

In order to convert the results obtained from CFD simulations into meaningful data and compare the performances of the heat exchangers, some further calculations are required. In the calculations made in such studies, the following equations and simplifications are generally applied in the literature.

Amount of heat transferred from each fluid can be calculated as in Eq. (12) and Eq (13) and then their mean can be taken to find average heat transfer rate by Eq. (14). These calculations utilize the average specific heat capacities (C_p) over the corresponding temperature range.

$$\dot{Q}_{hot} = \dot{m}_{hot} \cdot c_{p,hot} \cdot (T_{hot,in} - T_{hot,out}) \quad (12)$$

$$\dot{Q}_{cold} = \dot{m}_{cold} \cdot c_{p,cold} \cdot (T_{cold,out} - T_{cold,in}) \quad (13)$$

$$\dot{Q}_{ave} = (\dot{Q}_{hot} + \dot{Q}_{cold}) / 2 \quad (14)$$

For calculation of heat exchanger effectiveness value, the following equation is used:

$$\epsilon = \frac{\dot{Q}}{\dot{Q}_{max}} = \frac{C_{hot} (T_{hot,in} - T_{hot,out})}{C_{min} (T_{hot,in} - T_{cold,in})} = \frac{C_{cold} (T_{cold,out} - T_{cold,in})}{C_{min} (T_{hot,in} - T_{cold,in})} \quad (15)$$

where C_{hot} and C_{cold} represent heat capacity rate of hot and cold fluids and C_{min} is the lower one of those values. Heat capacity rates are calculated by Eqs. (16) and (17).

$$C_{hot} = \dot{m}_{hot} \cdot c_{p,hot} \quad (16)$$

$$C_{cold} = \dot{m}_{cold} \cdot c_{p,cold} \quad (17)$$

Overall Heat Transfer Coefficient (U) which is defined by Eq. (18) is an important parameter for evaluating a heat exchanger's thermal performance.

$$U = \frac{\dot{Q}}{A (\Delta T_{LMTD})} \quad (18)$$

In Eq. (18), A is the total surface area of the contact region where heat transfer takes place and ΔT_{LMTD} stands for Logarithmic Mean Temperature Difference. ΔT_{LMTD} can be attained by following steps given with Eq. (19 a,b,c):

$$\Delta T_{LMTD} = \frac{\Delta T_A - \Delta T_B}{\ln\left(\frac{\Delta T_A}{\Delta T_B}\right)} \quad (19a)$$

$$\Delta T_A = T_{hot,in} - T_{cold,out} \quad (19b)$$

$$\Delta T_B = T_{hot,out} - T_{cold,in} \quad (19c)$$

On the other hand, there are some important dimensionless numbers in heat and flow phenomena. For the flow inside helically coiled tube, Re number can be calculated by Eq. (20) [9]:

$$Re_{coil} = 2100 \left[1 + 12 \left(\frac{D_{t,i}}{D_{coil}} \right)^{1/2} \right] \quad (20)$$

Dean number can be obtained utilizing Re number as follows:

$$De = Re_{coil} \left(\frac{D_{t,i}}{D_{coil}} \right)^{1/2} \quad (21)$$

The coil side Nusselt number can be found by Eq. (22) [8]:

$$Nu_{coil} = 0.0456 \left(\frac{D_{coil}}{D_{t,i}} \right)^{-0.16} Re_{coil}^{0.8} Pr_{coil}^{0.4} \quad (22)$$

General form of Reynolds number can be given as:

$$Re = \frac{\rho VD}{\mu} \quad (23)$$

Reynolds number for shell and coil side could be rewritten as follows:

$$Re_{shell} = \frac{4 \dot{m}_{shell}}{\pi D_{h,shell} \mu} \quad (24)$$

$$Re_{coil} = \frac{4 \dot{m}_{coil}}{\pi D_{t,i} \mu} \quad (25)$$

In Eq. (24) hydraulic diameter of shell side is calculated as:

$$D_{h,shell} = \frac{4 \times \text{Volume of shell side domain}}{\text{Contact surface with fluid}} \quad (26)$$

The Nusselt number for the Shell side can be calculated by Eq. (27) and Eq. (28) [9].

$$Nu_{shell} = 0.6 Re_{shell}^{0.5} Pr_{shell}^{0.31} \quad \text{for } 50 < Re < 10000 \quad (27)$$

$$Nu_{shell} = 0.224 Re_{shell}^{0.6} Pr_{shell}^{0.33} \quad \text{for } 6000 < Re < 10000 \quad (28)$$

Alternatively Nusselt number of each side can be obtained in terms of hydraulic diameters as follows:

$$Nu_{coil} = \frac{h_i D_{t,i}}{k} \quad (\text{Since } D_{h,coil} = D_{t,i}) \quad (29)$$

$$Nu_{shell} = \frac{h_{shell} D_{h,shell}}{k} \quad (30)$$

5. Results

5.1. CFD simulation results

The simulations were carried out using ANSYS Fluent with the two designs described above. Within the scope of simulations steady state conditions were assumed and $k-\epsilon$ turbulence model was used. It was assumed that the cold fluid enters to the shell side and hot fluid is

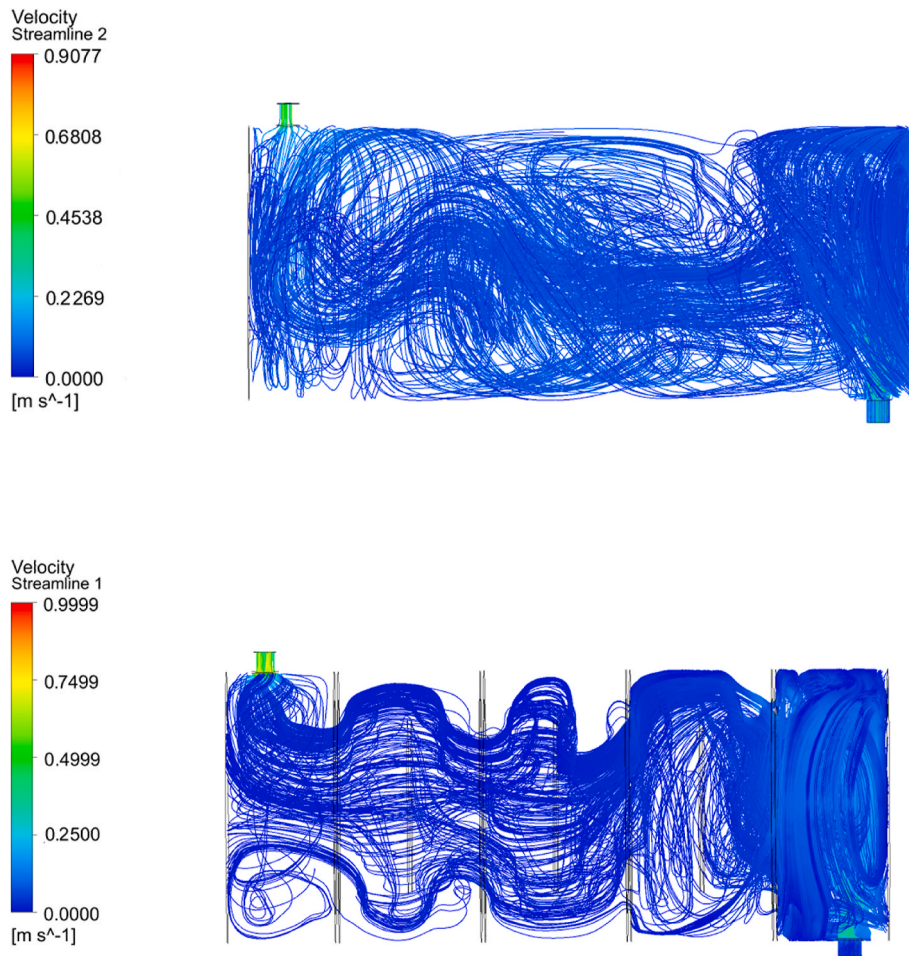


Fig. 10. Streamlines in the conventional and modified SHCTHEXs.

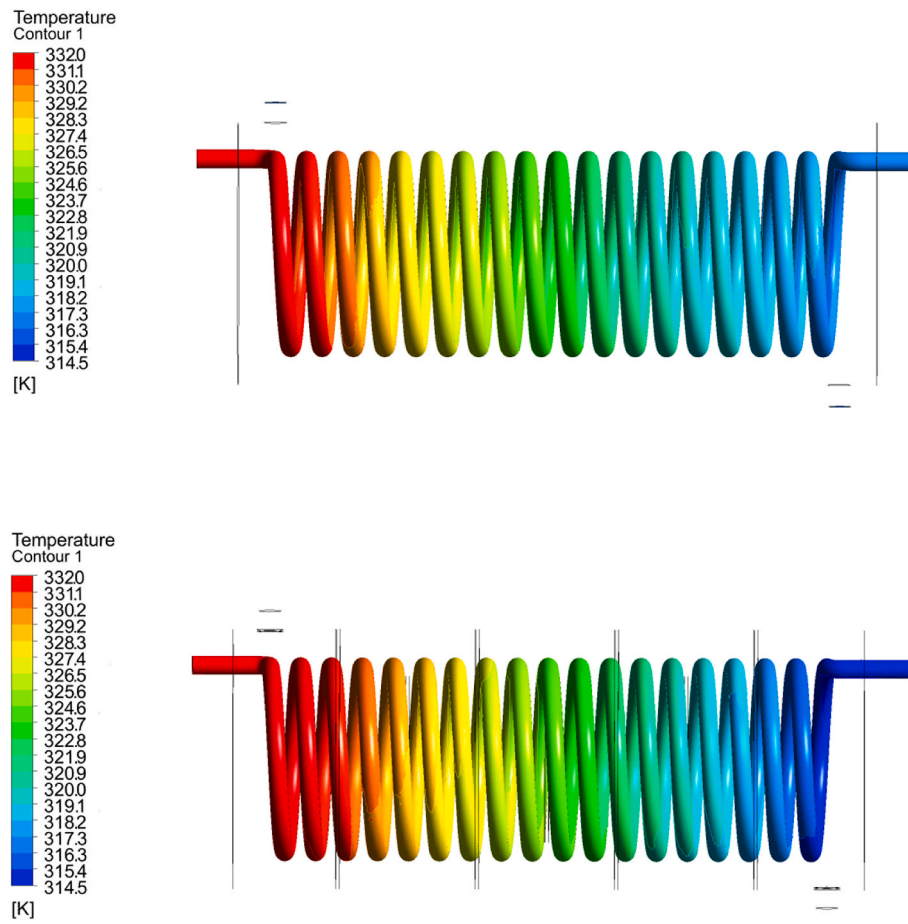


Fig. 11. Temperature variation in the hot side of conventional and modified heat exchangers.

circulated at the coil side. Water (liquid) was chosen as the fluid for both sides, its properties were selected from the Fluent database. In the simulations, cold water entered the shell side at 291.65 K and hot water entered the tubes at 333.15 K. At first step of numerical study, initial simulations with different temperature ranges have been conducted to determine the general performance of heat exchangers. Then, numerical simulations have been repeated regarding to the experimentally determined inlet temperatures. It was assumed that the hot water flowed at a flow rate of 3 l/min (liters/minute) and keeping this constant, the cold water flow rate was changed between 2 and 6 l/min with increments of 1 l/min. The same process is repeated for 4 l/min hot water flow rate.

Streamline is the path that a fluid particle follows throughout the flow field. It gives an insight about the general flow structure and widely used to estimate the performance of new designs involving fluid flow. Fig. 10 shows the streamlines of the conventional SHCTHEX and the modified SHCTHEX with circular baffles. The streamlines of the modified shell and helically coiled heat exchanger reveal that the fluid particles are forced to travel a desired path with diversions around the coiled tube because of the rings and discs. This flow structure enhances the turbulent effects and increases the amount of fluid particles in contact with the helically coiled tube. On the other hand, most of the fluid particles seem to be following a path through the tube's inner void in conventional heat exchanger.

Heat exchangers are used to transfer heat from one source to another. Temperature difference between inlet and outlet is one of the most

important indicators to evaluate their performance. Thanks to CFD simulations it is also possible to reveal the temperature distributions along the streams and in this way a good comparison of different designs can be made. Fig. 11 shows the hot side temperature contours of conventional shell and helically coiled heat exchanger and the modified one (both streams at 3 l/min). The temperature contours are presented with the same temperature intervals and the color distributions reveal that hot fluid cools down better with the modified heat exchanger. In other words, a cooler outlet temperature is seen in the temperature distribution of the modified heat exchanger in comparison with conventional one which means high heat transfer to the cold side. It is possible to say that the discs and rings create turbulent flows that improves heat transfer by increasing the convective heat transfer.

Fig. 12 shows the cold side temperature contours of conventional shell and helically coiled heat exchanger and the modified one on longitudinal cross-section plane (both streams at 3 l/min). Looking at Fig. 12, the temperature gradients are remarkable in modified heat exchanger and it can be easily seen how heat is carried away from the coiled pipe to shell side fluid. The obtained temperature contours are in harmony with the streamline formation of that design. On the other hand, although temperature increases incrementally from inlet to outlet, temperature gradients are hardly visible in the conventional heat exchanger. This phenomenon is also visualized in 3 dimensions in Fig. 13. The 3-dimensional temperature gradients formed around the coil are clearly visible in the modified heat exchanger. Temperature

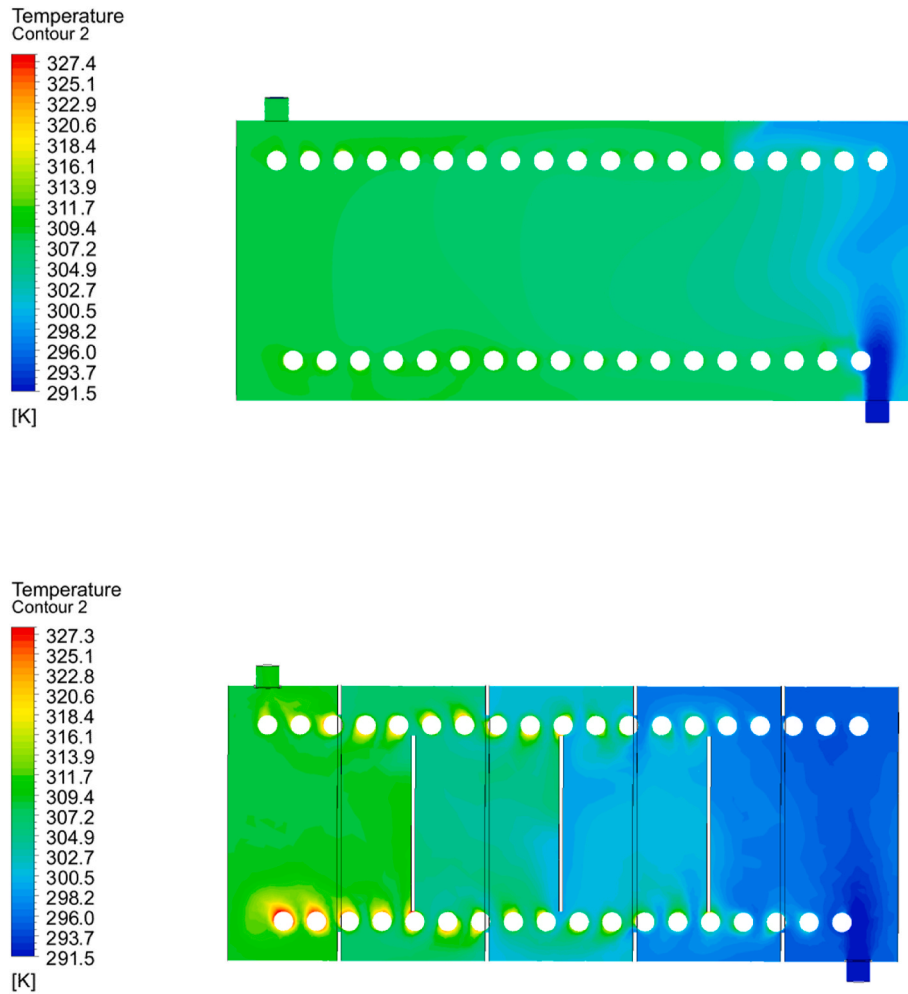


Fig. 12. Temperature variation in the cold side of conventional and modified heat exchangers on longitudinal cross-section plane.

volume renderings of conventional and modified heat exchangers obviously illustrates the main difference between heat transfer processes in both systems.

The general purpose of a heat exchanger is to transfer heat from one medium to another. In heat transfer processes without phase change, the temperature differences between the inlet and outlet of the flows, and hence the outlet temperatures, are important indicators of the performance of a heat exchanger. Fig. 14 shows hot fluid outlet temperatures of conventional heat exchanger and modified heat exchanger with varying cold fluid flow rates at two different hot fluid flow rates. As clearly seen in Fig. 14, hot fluid's outlet temperatures in modified SHCTHEX are lower than that of unmodified SHCTHEX at all flow rates which means better heat transfer in heat exchanger with baffles. According to the simulations, the modified heat exchanger provides 0.9–1.6 K better cooling than the conventional one.

Fig. 15 shows cold fluid outlet temperatures of conventional heat exchanger and modified heat exchanger with varying cold fluid flow rates at two hot fluid rates. Analyzing Fig. 15 indicates that, cold fluid outlet temperatures of modified system at all flow rates are higher than outlet temperatures of unmodified one. It can be said that the cold fluid absorbs more heat and its outlet temperatures are 0.6–1.9 K higher in modified heat exchanger.

It should be stated that the modified heat exchanger illustrated better performance in terms of outlet temperatures according to simulations outcomes. The improvement in outlet temperatures is also an indication of the improvement in heat transfer.

The amount of average heat transfer is an important factor in evaluation of heat exchanger performance and can be calculated as described in section 5 by utilizing the differences in inlet and outlet temperatures. Fig. 16 shows the calculated amounts of average heat transfer with respect to increasing cold fluid flow rate at two different hot flow rates for the simulated two designs. It can be concluded that the modified heat exchanger provided a better heat exchange. The average amount of heat transfer of conventional design varied between 2950 and 4400 W, whereas this parameter varied between 3100 and 4650 W for the modified heat exchanger at 3 l/min hot fluid flow rate. Also, calculated values of average amount of heat transfer for conventional and modified heat exchangers varied between 3120–5050 W and 3380–5310 W, respectively at 4 l/min hot fluid flow rate. Average amount of increase in average heat transfer rate was calculated as 7.05% and 7.1% respectively, for simulations at 3 l/min and 4 l/min hot fluid flow rates.

Overall heat transfer coefficient is another important parameter in heat exchanger design and can be described as a measure of how well

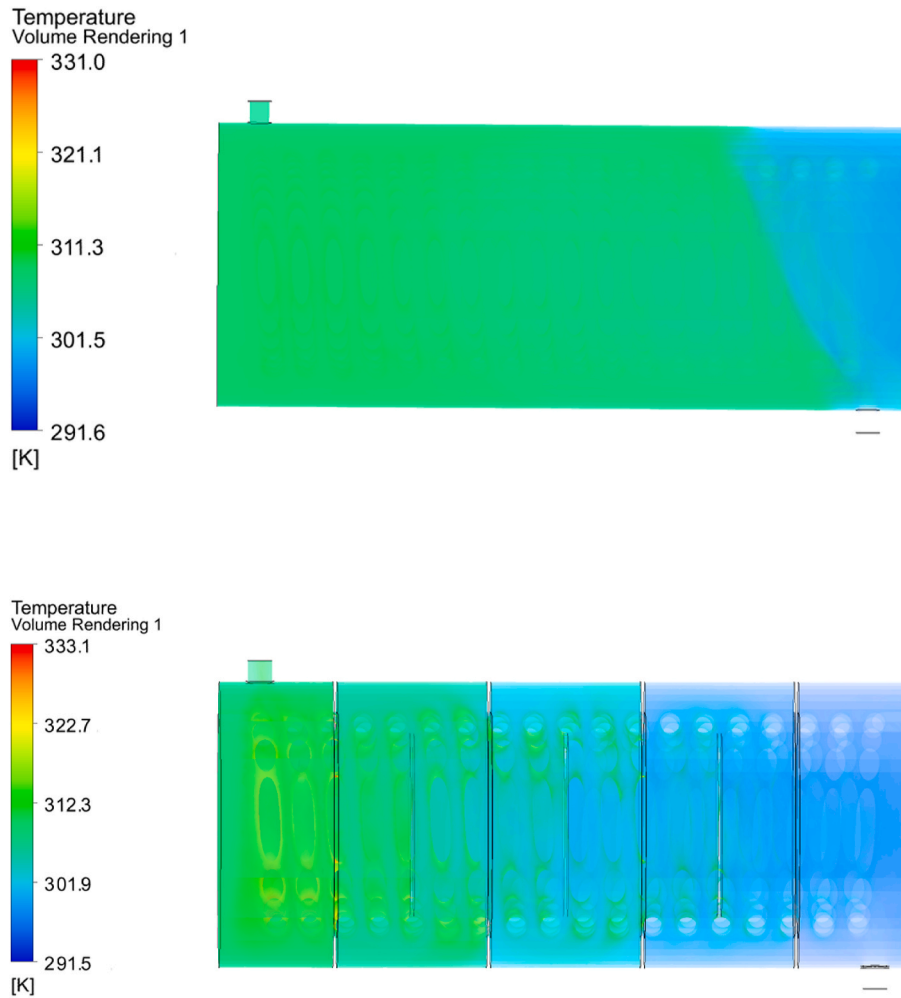


Fig. 13. Temperature volume rendering in cold side of conventional and modified heat exchangers.

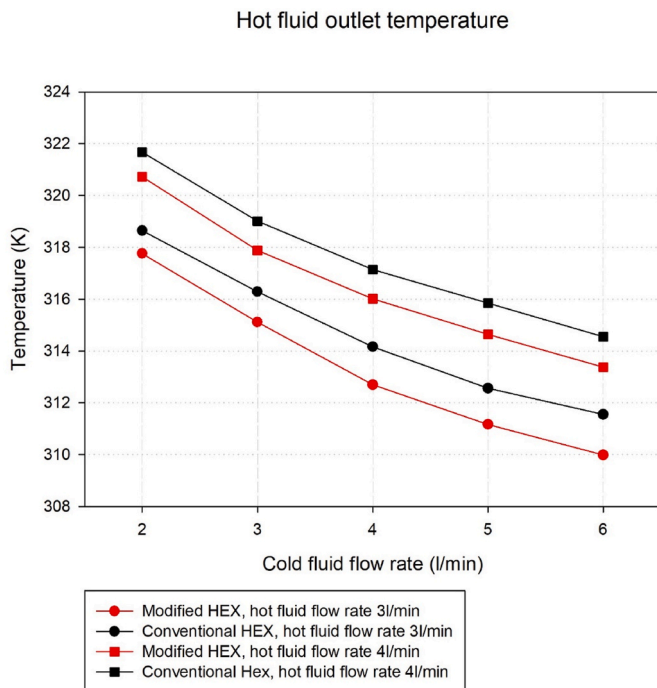


Fig. 14. Outlet temperatures of hot side with respect to the flow rate.

heat is transferred in contact areas of heat exchangers. Fig. 17 shows the calculated overall heat transfer values of the conventional and the modified heat exchangers with increasing cold fluid flow at two different hot fluid flow rates. Calculated values of overall heat transfer coefficients of conventional heat exchanger are between 800 and 1160 W/m². K and they are between 1050 and 1350 W/m². K for the modified heat exchanger at 3 l/min hot fluid flow rate. At 4 l/min hot fluid flow rate, overall heat transfer coefficient values of conventional heat exchanger are between 885 and 1210 W/m². K and they are between 1135 and 1390 W/m². K for the modified heat exchanger. The results indicate a 22.1% average increase in overall heat transfer coefficient for 3 l/min hot fluid flow rate and 19.6% average increase for 4 l/min hot fluid flow rate.

Fig. 18 shows a comparison of convective heat transfer coefficients calculated for conventional heat exchanger and modified heat exchanger. Calculated values of convective heat transfer coefficients of conventional heat exchanger are between 1090 and 2180 W/m². K and they are between 1350 and 2700 W/m². K for the modified heat exchanger. With the modifications made, an average increase of 24% is obtained in convective heat transfer coefficient.

Fig. 19 presents numerically obtained pressure drop values in conventional and modified SHCTHEXs with respect to flow rate. As it can be seen, adding baffles increased pressure drop in the cold side of the SHCTHEX. The highest increment in the pressure drop of the shell side was determined as 16% by adding baffles. In a study performed by Tuncer et al. [22]; pressure drop in shell side of finless and finned SHCTHEXs at 3 lpm were numerically calculated as 681 Pa and 817 Pa,

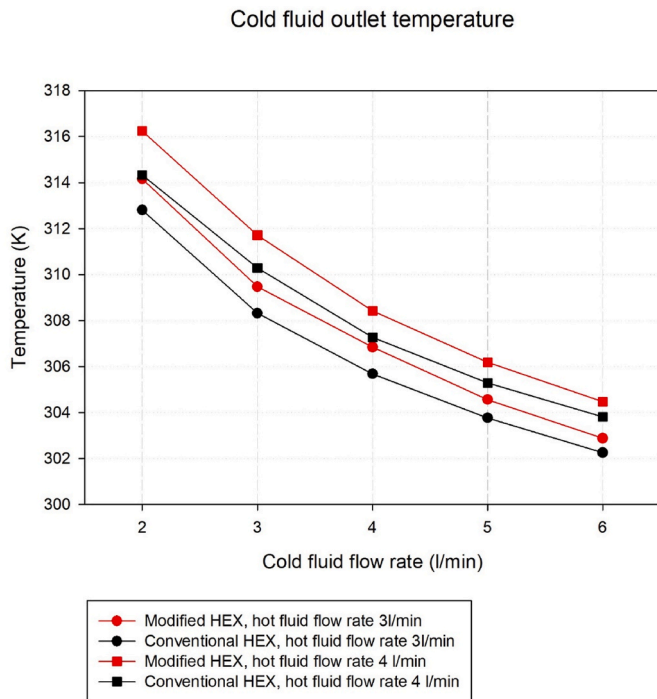


Fig. 15. Outlet temperature of cold side with respect to the flow rate.

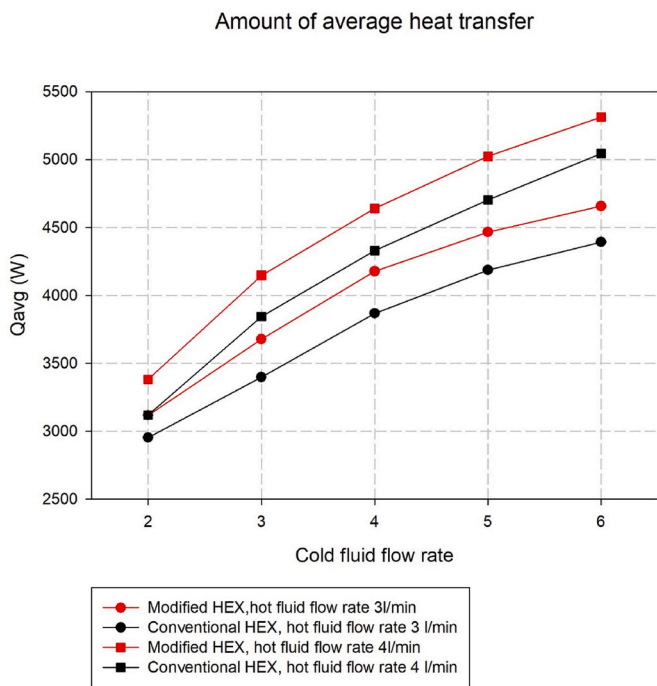


Fig. 16. Average heat transfer rate with respect to the flow rate.

respectively. Xu et al. [55] numerically investigated a shell and helically coiled spiral grooved heat exchanger and obtained pressure drop approximately between 20 and 2000 Pa. Wang et al. [56] simulated a shell and helically coiled spiral grooved heat exchanger and calculated pressure drop approximately in the range of 50–2100 Pa. Andrzejczyk and Muszynski [5] experimentally investigated a SHCTHEX with core-baffle modification and achieved pressure drop between 600 and 1200 Pa. Their results also showed that using baffles in the shell side increased pressure drop. Obtained numerical results of pressure drop of

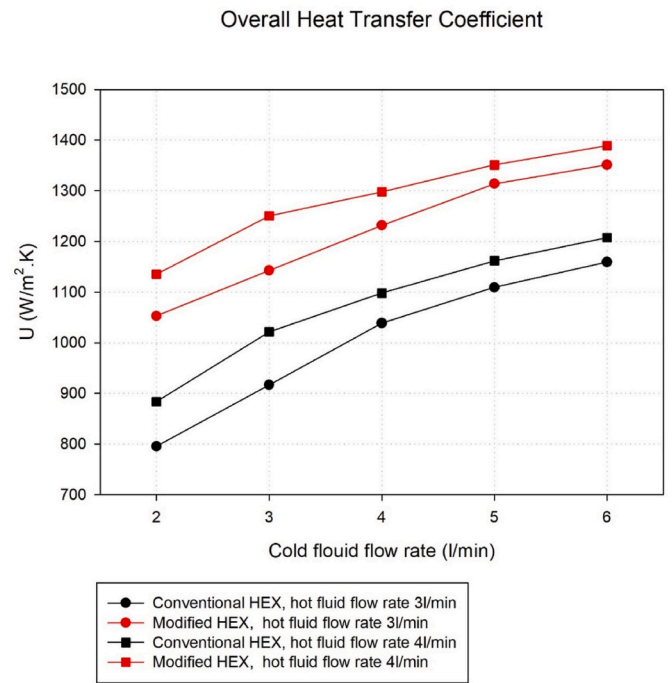


Fig. 17. Overall heat transfer coefficient variation with respect to the flow rate.

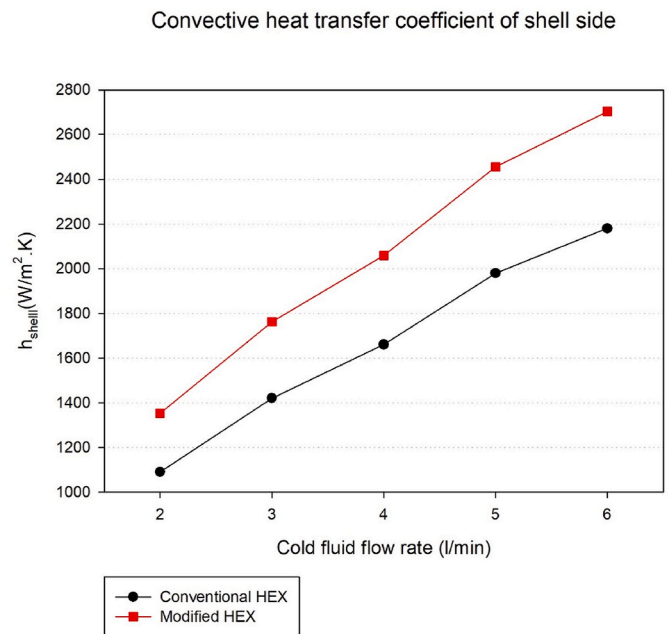


Fig. 18. Convective heat transfer coefficient variation with respect to the flow rate.

the heat exchanger designs in this study, is in acceptable range when compared to related numerical and experimental studies which investigated similar SHCTHEXs. It is better to state that, the achieved pressure drop values in this study are lower compared to the given studies. In the presented studies complex designs for SHCTHEXs, restricts the flow significantly which led to obtain higher pressure drop values. However, with the baffled design proposed in this work, thermal performance of SHCTHEX improved significantly by guiding the flow over the coiled tube while the pressure drop was kept in acceptable range.

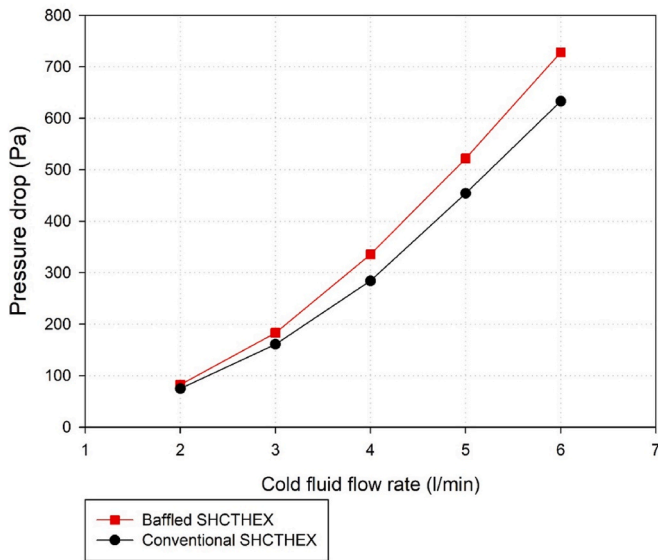


Fig. 19. Pressure drop values in conventional and modified SHCTHEX with respect to flow rate.

5.2. Experimental results

After the simulations, experiments are performed with the setup shown in Figs. 8 and 9. Fig. 20 presents the hot fluid outlet temperatures of modified heat exchanger, obtained by simulations and experiments. Simulations indicated better results, however close values were measured at experiments. A maximum of 0.57 K and an average of 0.43 K difference between experimental and simulation values was noted at 4 l/min hot fluid flow rate. The maximum and average difference between experimental and numerical outlet temperature for 3 l/min hot fluid flow rate obtained as 0.59 K and average 0.32 K, respectively.

Fig. 21 shows the cold fluid outlet temperatures of modified heat exchanger, gained by simulations and experiments. The obtained

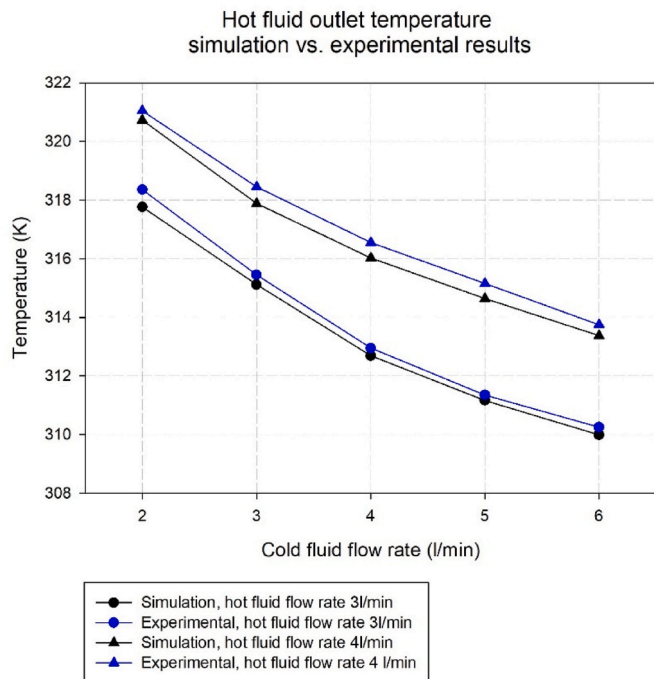


Fig. 20. Hot side's outlet temperature variation with respect to the cold flow rate at two different flow rate of hot side.

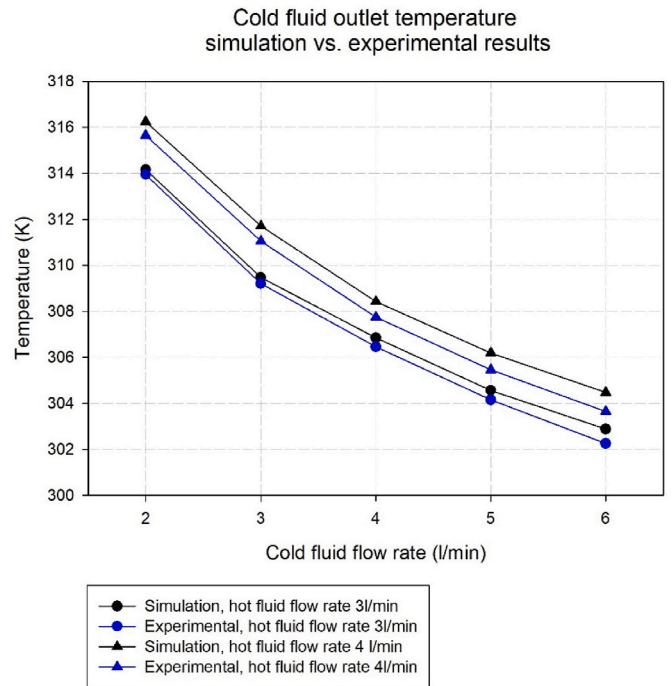


Fig. 21. Cold side's outlet temperature variation with respect to the cold flow rate at two different flow rate of hot side.

outcomes for cold side outlet temperature showed that simulations gave better results. In the experiments performed with 3 l/min hot fluid flow, the experimental values of the cold fluid outlet temperature were found to be 0.62 K lower at the maximum and 0.38 K on average compared to the simulation values. Those values were 0.81 K at maximum and 0.69 K on average for 4 l/min hot fluid flow rate. Also, Fig. 21 reveals that as the cold fluid flow rate increases, the temperature differences increase.

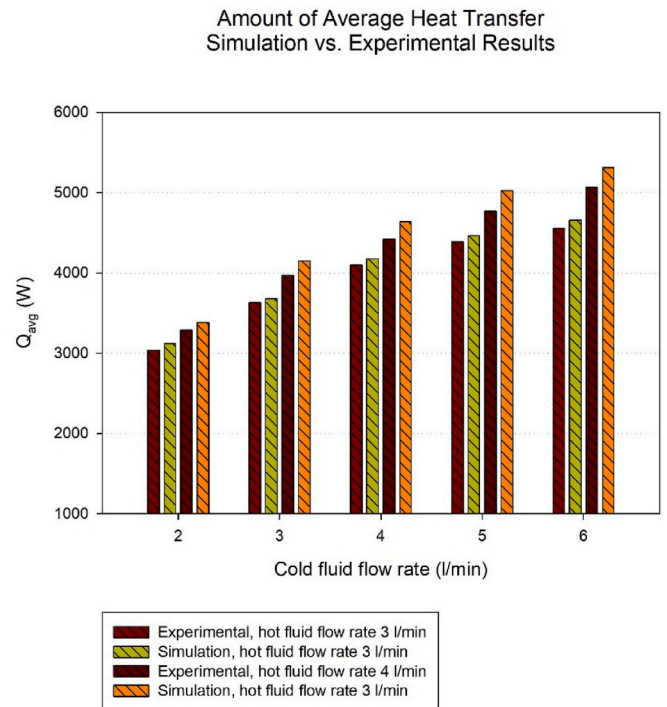


Fig. 22. Average heat transfer rate variation with respect to the cold flow rate at two different flow rate of hot side.

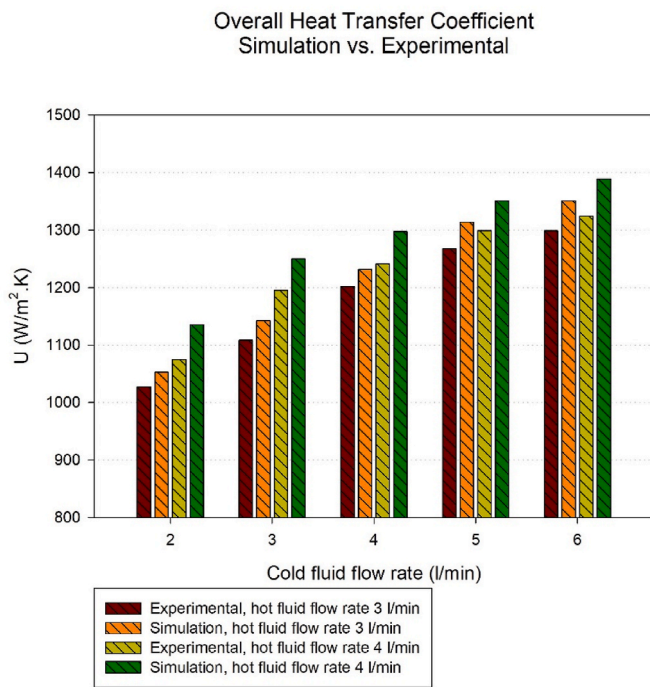


Fig. 23. Overall heat transfer coefficient variation with respect to the cold flow rate at two different flow rate of hot side.

This shows that the outlet temperatures were effected by the dominant stream.

The differences in outlet temperatures are in favor of simulations as expected. This is mostly the case because the simulation approach presents idealized versions of real systems. On the other hand, it is impossible to create an adiabatic medium in the experiments. Although there was a certain amount of insulation on the heat exchanger and its connections, still there might have been some heat loss to the surroundings.

With these measurements, amounts of average heat transfer were calculated and compared with simulation results. Fig. 22 represents the amount of heat transfer calculated utilizing simulation and experimental results. The average differences between simulation and experimental values in terms of average amount of heat transfer rate obtained as 2.4% for 3 l/min hot fluid flow rate and 3.5% for 4 l/min hot fluid flow rate.

Fig. 23 illustrates numerically and experimentally attained overall

heat transfer coefficient with respect to the cold flow rate at two different flow rate of hot side. The amount of differences in calculated overall heat transfer coefficient values between simulation and experimental results obtained as 3.16% for 3 l/min hot fluid flow rate and 4.76% for 4 l/min hot fluid flow rate. In this study, overall heat transfer coefficient of modified SHCTHEX with circular baffles achieved in the range of 1050–1400 W/m²K. In a study Bahrehmand and Abbassi [57] developed and experimentally examined a SHCTHEX and attained overall heat transfer coefficient of approximately in the range of 1000–1550 W/m²K. In another study done by Niwalkar et al. [58]; SHCTHEX was tested by using water and nanofluid and overall heat transfer coefficient approximately achieved between 700 and 2800 W/m²K. Moreover, in a research performed by Kumar et al. (2018) overall heat transfer coefficient of a SHCTHEX by using water and nanofluid as working fluids was determined between the range of 500–3500 W/m²K.

Table 4 represents a comparison between the outcomes of this research and related works on SHCTHEXs. In Table 4, various factors like flow rate, Reynolds number, heat transfer rate and heat transfer coefficient are presented. As known, the given parameters are important in evaluating heat exchangers. A general and detailed comparison between the outcomes of this work and the results of related studies clearly indicates a good agreement between them. However, it is better to state that geometrical parameters of the given SHCTHEXs and test conditions are not the same. This phenomenon makes it hard to conduct a sensitive comparison among the given works. But in general, it can be concluded that the findings of this research are in line with the related works available in the literature.

6. Conclusions

In this study CFD approach was utilized to reveal the performance of a new SHCTHEX design comparing it with the conventional design. Then the modified heat exchanger was fabricated and experimentally analyzed as well. According to the streamlines and temperature contours obtained by simulations, the baffled heat exchanger design created better contact of fluids at contact regions and heat was transferred in a more effective way in comparison to conventional one. In other words, modified heat exchanger provided a better heat exchange when parameters like outlet temperatures and heat transfer rates compared. Average amount of increase in mean heat transfer rate was calculated as 7.05% and 7.1%, respectively for simulations at 3 l/min and 4 l/min hot fluid flow rates. The findings indicated a 22.1% average increase in

Table 4
A comparison between the outcomes of this research and related works on SHCTHEXs.

Ref.	Method		Volume/mass flow rate	Re _{coil}	Re _{shell}	Heat transfer rates (W)	h _{coil} (W/m²K)	h _{shell} (W/m²K)	U (W/m²K)
	Exp	Num							
Barzegari et al. [59]	✓	-	2 – 3.5 l/min	10800 – 21182	-	2200 – 9500	2150 – 3000	-	-
Tuncer et al. [2],	✓	✓	1.5 – 3.5 l/min	6600 – 16000	~ 600 – 1100	2000 – 4600	5700 – 13400	2250 – 4050	1600 – 3150
Tuncer et al. [2],	✓	✓	1.5 – 3.5 l/min	6600 – 16000	~ 600 – 1100	1940 – 5180	5670 – 15000	2250 – 4670	1600 – 3530
Naik and Vinod [60]	✓	-	0.5 – 5 l/min	-	-	-	-	-	500 – 3500
Jamshidi et al. [4]	✓	-	1 – 4 l/min	2000 – 1000	-	-	-	-	625 – 1100
Alimoradi et al. [61]	-	✓	-	-	7500 – 15000	~ 3500 – 8000	2671(optimum)	-	-
Zaboli et al. [62]	-	✓	-	~ 14000 – 23000	-	-	~ 8700 – 11400	-	-
Zaboli et al. [63]	-	✓	1 – 4 l/min	1300 – 5270	-	-	500 – 3000	-	-
Elshazly et al. [54]	✓	-	1.7 – 11.15 l/min	5700 – 55000	-	-	2000 – 2700	-	500 – 2000
Niwalkar et al. [58]	✓	-	0.5 – 0.84 l/min	1500 – 4200	-	-	2000 – 14000	-	800 – 2800
Panahi, and Zamzamin [21]	✓	-	1 – 5 l/min	4000 – 18000	-	-	-	-	400 – 1700
Bahrehmand and Abbassi [57]	-	✓	0.3 – 0.113 kg/s	10000 – 35000	-	3500 – 14000	5000 – 25000	1100 – 1500	1000 – 1550
Salem et al. [64]	✓	-	1.7 – 11 l/min	10000 – 60000	-	-	-	-	200 – 1500
This study	✓	✓	2 – 6 l/min	10600 – 14200	450 – 1950	2950 – 5350	5200 – 6500	1090 – 2700	800 – 1400

overall heat transfer coefficient for 3 l/min hot fluid flow rate and 19.6% average increase for 4 l/min hot fluid flow rate. Finally numerically obtained results for modified heat exchanger were verified by experimental findings. The average differences between simulation and experimental values in terms of average amount of heat transfer rate were obtained as 2.4% for 3 l/min hot fluid flow rate and 3.5% for 4 l/min hot fluid flow rate. Similarly, the amount of differences in calculated overall heat transfer coefficient values between simulation and experimental results were found to be 3.16% for 3 l/min hot fluid flow rate and 4.76% for 4 l/min hot fluid flow rate. The overall findings of this study exhibited the potential of adding baffles including discs and rings in improving the thermal performance of the SHCTHEX. In future studies, different nanofluids could be tested as working fluid to obtain more thermal improvement.

Declaration of competing interest

The authors declare that they have no known competing financial interests or personal relationships that could have appeared to influence the work reported in this paper.

Data availability

Data will be made available on request.

References

- P. Naphon, Thermal performance and pressure drop of the helical-coil heat exchangers with and without helically crimped fins, *Int. Commun. Heat Mass Tran.* 34 (2007) 321–330.
- A.D. Tuncer, A. Sözen, A. Khanlari, E.Y. Gürbüz, H.I. Variyenli, Analysis of thermal performance of an improved shell and helically coiled heat exchanger, *Appl. Therm. Eng.* 184 (2021), 116272.
- M.M. Etghani, S.A. Hosseini Baboli, Numerical investigation and optimization of heat transfer and exergy loss in shell and helical tube heat exchanger, *Appl. Therm. Eng.* 121 (2017) 294–301.
- N. Jamshidi, M. Farhadi, D.D. Ganji, K. Sedighi, Experimental analysis of heat transfer enhancement in shell and helical tube heat exchangers, *Appl. Therm. Eng.* 51 (2013) 644–652.
- R. Andrzejczyk, T. Muszynski, An experimental investigation on the effect of new continuous core-baffle geometry on the mixed convection heat transfer in shell and coil heat exchanger, *Appl. Therm. Eng.* 136 (2018) 237–251.
- A. Alimoradi, Investigation of exergy efficiency in shell and helically coiled tube heat exchangers, *Case Stud. Therm. Eng.* 10 (2017) 1–8.
- A. Alimoradi, Study of thermal effectiveness and its relation with NTU in shell and helically coiled tube heat exchangers, *Case Stud. Therm. Eng.* 9 (2017) 100–107.
- B.K. Hardik, P.K. Baburajan, S.V. Prabhu, Local heat transfer coefficient in helical coils with single phase flow, *Int. J. Heat Mass Tran.* 89 (2015) 522–538.
- R. Ramesh, S.N. Murugesan, C. Narendran, R. Saravanan, Experimental investigations on shell and helical coil solution heat exchanger in NH₃-H₂O vapour absorption refrigeration system (VAR), *Int. Commun. Heat Mass Tran.* 87 (2017) 6–13.
- H.M. Maghrabie, M. Attalla, A.A. Mohsen, Performance of a shell and helically coiled tube heat exchanger with variable inclination angle: experimental study and sensitivity analysis, *Int. J. Therm. Sci.* 164 (2021), 106869.
- H.M. Maghrabie, M. Attalla, A.A. Mohsen, Performance assessment of a shell and helically coiled tube heat exchanger with variable orientations utilizing different nanofluids, *Appl. Therm. Eng.* 182 (2021), 116013.
- S. Khorasani, A. Moosavi, A. Dadvand, M. Hashemian, A comprehensive second law analysis of coil side air injection in the shell and coiled tube heat exchanger: an experimental study, *Appl. Therm. Eng.* 150 (2019) 80–87.
- A.K. Solanki, R. Kumar, Condensation of R-134a inside dimpled helically coiled tube-in-shell type heat exchanger, *Appl. Therm. Eng.* 129 (2018) 535–548.
- F. Mebarek-Oudina, R. Fares, A. Aissa, R.W. Lewis, N.H. Abu-Hamdeh, Entropy and convection effect on magnetized hybrid nano-liquid flow inside a trapezoidal cavity with zigzagged wall, *Int. Commun. Heat Mass Tran.* 125 (2021), 105279.
- R. Kurian, C. Balaji, S.P. Venkateshan, Experimental investigation of near compact wire mesh heat exchangers, *Appl. Therm. Eng.* 108 (2016) 1158–1167.
- F. Afshari, H.G. Zavaragh, G. Di Nicola, Numerical analysis of ball-type turbulators in tube heat exchangers with computational fluid dynamic simulations, *Int. J. Environ. Sci. Technol.* 16 (2019) 3771–3780.
- N. Bianco, M. Iasiello, G.M. Mauro, L. Pagano, Multi-objective optimization of finned metal foam heat sinks: tradeoff between heat transfer and pressure drop, *Appl. Therm. Eng.* 182 (2021), 116058.
- F. Afshari, A. Sözen, A. Khanlari, A.D. Tuncer, Heat transfer enhancement of finned shell and tube heat exchanger using Fe₂O₃/water nanofluid, *J. Cent. S. Univ.* 28 (11) (2021) 3297–3309.
- N. Benarji, C. Balaji, S.P. Venkateshan, Optimum design of cross-flow shell and tube heat exchangers with low fin tubes, *Heat Tran. Eng.* 29 (10) (2008) 864–872.
- R. Andrzejczyk, T. Muszynski, M. Gosz, Experimental investigations on heat transfer enhancement in shell coil heat exchanger with variable baffles geometry, *Chem. Eng. Process: Process Intensif.* 132 (2018) 114–126.
- D. Panahi, K. Zamzamin, Heat transfer enhancement of shell-and-coiled tube heat exchanger utilizing helical wire turbulator, *Appl. Therm. Eng.* 115 (2017) 607–615.
- A.D. Tuncer, A. Sözen, A. Khanlari, E.Y. Gürbüz, H.I. Variyenli, Upgrading the performance of a new shell and helically coiled heat exchanger by using longitudinal fins, *Appl. Therm. Eng.* 191 (2021), 116876.
- A.K. Solanki, R. Kumar, Two-phase flow condensation heat transfer characteristic of R-600a inside the horizontal smooth and dimpled helical coiled tube in shell type heat exchanger, *Int. J. Refrig.* 107 (2019) 155–164.
- R. Andrzejczyk, T. Muszynski, Thermodynamic and geometrical characteristics of mixed convection heat transfer in the shell and coil tube heat exchanger with baffles, *Appl. Therm. Eng.* 121 (2017) 115–125.
- F. Afshari, Experimental and numerical investigation on thermoelectric coolers for comparing air-to-water to air-to-air refrigerators, *J. Therm. Anal. Calorim.* 144 (2021) 855–868.
- M. Iasiello, N. Bianco, W.K.S. Chiu, V. Naso, The effects of variable porosity and cell size on the thermal performance of functionally-graded foams, *Int. J. Therm. Sci.* 160 (2021), 106696.
- S.P. Pathak, K. Velusamy, K.K. Rajan, C. Balaji, Numerical and experimental investigations of heat removal performance of sodium-to-air heat exchanger used in fast reactors, *Heat Tran. Eng.* 36 (5) (2015) 439–451.
- P. Nithiarasu, R.W. Lewis, K.N. Seetharamu, *Fundamentals of the Finite Element Method for Heat and Mass Transfer*, John Wiley and Sons Ltd, Chichester, 2016.
- A. Andreozzi, N. Bianco, M. Iasiello, V. Naso, Numerical study of metal foam heat sinks under uniform impinging flow, *J. Phys. Conf. Ser.* 796 (2017), 012002.
- E. Çiftçi, A. Sözen, Heat transfer enhancement in pool boiling and condensation using h-BN/DCM and SiO₂/DCM nanofluids: experimental and numerical comparison, *Int. J. Numer. Methods Heat Fluid Flow* 31 (2020) 26–52.
- M. Miansari, M.R. Darvishi, D. Toghraie, P. Barnoon, M. Shirzad, A.A. Alizadeh, Numerical investigation of grooves effects on the thermal performance of helically grooved shell and coil tube heat exchanger, *Chin. J. Chem. Eng.* 44 (2022) 424–434, <https://doi.org/10.1016/j.cjche.2021.05.038>.
- E.P. Kumar, A.K. Solanki, M.M.J. Kumar, Numerical investigation of heat transfer and pressure drop characteristics in the micro-fin helically coiled tubes, *Appl. Therm. Eng.* 182 (2021), 116093.
- N.H. Abu-Hamdeh, K.H. Almitani, A. Alimoradi, Exergetic performance of the helically coiled tube heat exchangers: comparison the sector-by-sector with tube in tube types, *Alex. Eng. J.* 60 (2021) 979–993.
- M. Omid, M. Farhadi, A.A. Rabienataj Darzi, Numerical study of heat transfer on using lobed cross sections in helical coil heat exchangers: effect of physical and geometrical parameters, *Energy Convers. Manag.* 176 (2018) 236–245.
- G. Wang, T. Dbouk, D. Wang, Y. Pei, X. Peng, H. Yuan, S. Xiang, Experimental and numerical investigation on hydraulic and thermal performance in the tube-side of helically coiled-twisted trilobal tube heat exchanger, *Int. J. Therm. Sci.* 153 (2020), 106328.
- H. Mirgolbabaee, Numerical investigation of vertical helically coiled tube heat exchangers thermal performance, *Appl. Therm. Eng.* 136 (2018) 252–259.
- A. Alimoradi, F. Veysi, Prediction of heat transfer coefficients of shell and coiled tube heat exchangers using numerical method and experimental validation, *Int. J. Therm. Sci.* 107 (2016) 196–208.
- N.H. Abu-Hamdeh, R.A.R. Bantan, I. Tilili, Analysis of the thermal and hydraulic performance of the sector-by-sector helically coiled tube heat exchangers as a new type of heat exchangers, *Int. J. Therm. Sci.* 150 (2020), 106229.
- A. Güngör, A. Sözen, A. Khanlari, Numerical investigation of thermal performance enhancement potential of using Al₂O₃-TiO₂/water hybrid nanofluid in shell and helically coiled heat exchangers, *Heat Tran. Res.* 53 (12) (2022) 37–54.
- R.W. Lewis, P. Nithiarasu, K.N. Seetharamu, *Fundamentals of the Finite Element Method for Heat and Fluid Flow*, John Wiley and Sons Ltd, Chichester, 2004, <https://doi.org/10.1002/0470014164>.
- F. Afshari, A. Sözen, A. Khanlari, A.D. Tuncer, C. Şirin, Effect of turbulator modifications on the thermal performance of cost-effective alternative solar air heater, *Renew. Energy* 158 (2020) 297–310.
- F. Afshari, A. Khanlari, A.D. Tuncer, A. Sözen, I. Şahinkesen, G. Di Nicola, Dehumidification of sewage sludge using quonset solar tunnel dryer: an experimental and numerical approach, *Renew. Energy* 171 (2021) 784–798.
- E.Y. Gürbüz, A. Sözen, H.I. Variyenli, A. Khanlari, A.D. Tuncer, A comparative study on utilizing hybrid-type nanofluid in plate heat exchangers with different number of plates, *J. Braz. Soc. Mech. Sci. Eng.* 42 (2020) 524.
- E. Çiftçi, A. Khanlari, A. Sözen, I. Aytaç, A.D. Tuncer, Energy and exergy analysis of a photovoltaic thermal (PVT) system used in solar dryer: a numerical and experimental investigation, *Renew. Energy* 180 (2021) 410–423.
- A. Khanlari, A.D. Tuncer, A. Sözen, I. Aytaç, E. Çiftçi, H.I. Variyenli, Energy and exergy analysis of a vertical solar air heater with nano-enhanced absorber coating and perforated baffles, *Renew. Energy* 187 (2022) 586–602.
- ANSYS, *ANSYS Fluent Theory Guide*, ANSYS Inc, Canonsburg, 2017.
- S. Karagoz, F. Afshari, O. Yildirim, O. Comakli, Experimental and numerical investigation of the cylindrical blade tube inserts effect on the heat transfer enhancement in the horizontal pipe exchangers, *Heat Mass Tran.* 53 (9) (2017) 2769–2784.

- [48] M. Karagöz, Ü. Ağbulut, S. Sarıdemir, Waste to energy: production of waste tire pyrolysis oil and comprehensive analysis of its usability in diesel engines, *Fuel* 275 (2020), 117844.
- [49] A. Khanlari, D. Yılmaz Aydın, A. Sözen, M. Gürü, H.I. Variyenli, Investigation of the influences of kaolin-deionized water nanofluid on the thermal behavior of concentric type heat exchanger, *Heat Mass Tran.* 56 (2020) 1453–1462.
- [50] A. Khanlari, A.D. Tuncer, A. Sözen, C. Şirin, A. Gungor, Energetic, environmental and economic analysis of drying municipal sewage sludge with a modified sustainable solar drying system, *Sol. Energy* 208 (2020) 787–799.
- [51] A.D. Tuncer, A. Sözen, F. Afshari, A. Khanlari, C. Şirin, A. Gungor, Testing of a novel convex-type solar absorber drying chamber in dehumidification process of municipal sewage sludge, *J. Clean. Prod.* 272 (2020), 122862.
- [52] A.K. Solanki, R. Kumar, Condensation frictional pressure drop characteristic of R-600a inside the horizontal smooth and dimpled helical coiled tube in shell type heat exchanger, *Int. J. Therm. Sci.* 154 (2020), 106406.
- [53] S. Khorasani, A. Dadvand, Effect of air bubble injection on the performance of a horizontal helical shell and coiled tube heat exchanger: an experimental study, *Appl. Therm. Eng.* 111 (2017) 676–683.
- [54] K.M. Elshazly, R.Y. Sakr, R.K. Ali, M.R. Salem, Effect of γ -Al₂O₃/water nanofluid on the thermal performance of shell and coil heat exchanger with different coil torsions, *Heat Mass Tran.* 53 (2017) 1893–1903.
- [55] P. Xu, T. Zhou, J. Xing, J. Chen, Z. Fu, Numerical investigation of heat-transfer enhancement in helically coiled spiral grooved tube heat exchanger, *Prog. Nucl. Energy* 145 (2022), 104132.
- [56] G. Wang, A. Liu, T. Dbouk, D. Wang, X. Peng, A. Ali, Optimal shape design and performance investigation of helically coiled tube heat exchanger applying MO-SHERPA, *Int. J. Heat Mass Tran.* 184 (2022), 122256.
- [57] S. Bahreghmand, A. Abbassi, Heat transfer and performance analysis of nanofluid flow in helically coiled tube heat exchangers, *Chem. Eng. Res. Des.* 109 (2016) 628–637.
- [58] A.F. Niwalkar, J.M. Kshirsagar, K. Kulkarni, Experimental investigation of heat transfer enhancement in shell and helically coiled tube heat exchanger using SiO₂/water nanofluids, *Mater. Today Proc.* 18 (2019) 947–962.
- [59] H. Barzegari, A. Tavakoli, D. Jalali Vahid, Experimental study of heat transfer enhancement in a helical tube heat exchanger by alumina nanofluid as current flow, *Heat Mass Tran.* 55 (2019) 2679–2688.
- [60] B.A.K. Naik, A.V. Vinod, Heat transfer enhancement using non-Newtonian nanofluids in a shell and helical coil heat exchanger, *Exp. Therm. Fluid Sci.* 90 (2018) 132–142.
- [61] A. Alimoradi, M. Olfati, M. Maghareh, Numerical investigation of heat transfer intensification in shell and helically coiled finned tube heat exchangers and design optimization, *Chem. Eng. Process: Process Intensif.* 121 (2017) 125–143.
- [62] M. Zaboli, S. Saedodin, S.S. Mousavi Ajarostaghi, M. Nourbakhsh, Numerical evaluation of the heat transfer in a shell and corrugated coil tube heat exchanger with three various water based nanofluids, *Heat Transfer* 50 (6) (2021) 6043–6067.
- [63] M. Zaboli, S.S.M. Ajarostaghi, M. Noorbakhsh, Effects of geometrical and operational parameters on heat transfer and fluid flow of three various water based nanofluids in a shell and coil tube heat exchanger, *SN Appl. Sci.* 1 (2019) 1387.
- [64] M.R. Salem, K.M. Elshazly, R.Y. Sakr, R.K. Ali, Experimental investigation of coil curvature effect on heat transfer and pressure drop characteristics of shell and coil heat exchanger, *J. Therm. Sci. Eng. Appl.* 7 (2015), 011005.